UPPER BOUND ELEMENT TECHNIQUE (UBET) AS A DESIGN TOOL FOR RING ROLLING PROCESS

Adel Alfozan and **Jay S. Gunasekera,** Dept. of Mechanical Engineering, Ohio University, Athens, Ohio, USA. *E-mail*: gsekera@bobcat.ent.ohiou.edu

Abstract

The upper bound element technique (UBET) is used to determine the optimum intermediate shape for profile ring rolling using backward simulation. The lowest energy rate is the key issue in achieving the optimal intermediate shape as well as the backward simulation of the process. The plastic flow of material in ring rolling is assumed to be a sequence of successive closed-die forging processes. The ring is divided into features, which provide an approximated profile consisting of a number of rectangular elements. The simulation of the profile ring rolling was tested with different profiles of rolls, and two such cases are presented here. The present method was validated using an experimental radial ring rolling mill designed and fabricated in the Dept. of Mechanical Engineering at Ohio University for the investigation of both cold and hot ring rolling processes. As the results show, this technique is capable of solving the backward simulation of profile ring rolling problems in a much shorter time compared to the finite element method (FEM). This approach can be applied effectively to the profile ring rolling process and can serve as a useful tool in industrial applications.

Keywords: *Backward Simulation, Upper Bound Element Technique (UBET), Ring Rolling, Metal Forming*

Introduction

Ring rolling is a metal forming operation that reduces the thickness (cross section) and enlarges the diameter (circumference) of the workpiece by a squeezing action as it passes between two rotating rolls. The ring rolling process is widely used to produce seamless rings with outer diameters ranging from 100 mm up to 8 m with cold or hot workpieces [1]. These rings are commonly used as flanges, pipe flanges, ring gears, structural rings, gas-turbine rings, and so on. Titanium and superalloy rings are used as housing parts for jet engines in the aerospace industry. Advantages of the process are uniform quality, smooth surface finish, close tolerance, short production time and relatively small material loss [2], especially for rings of complex profiles. There are, however certain disadvantages in this process compared to forging. For example, ring rolling is poor in filling the roll cavities, especially when they are too deep, due to the fact that during the ring rolling process the cross-section of the ring is reduced, resulting in an enlargement of the diameter of the ring without adequate filling of the roll cavities.

A typical ring rolling process has two sets of rolls: the radial set reduces the radial thickness of the ring, whereas the axial set controls the height of the ring, as shown in *Figure 1*. During the ring rolling process, the main deformation occurs between the main (king) roll and the mandrel (pressure) roll. The rotation of the king roll, coupled by friction at the roll/ring interface, drives the ring through the roll gap. The wall thickening of the ring is continuously reduced by the advancing pressure roll [3]. As the cross-section of the ring is gradually reduced, the diameter of the ring grows progressively.

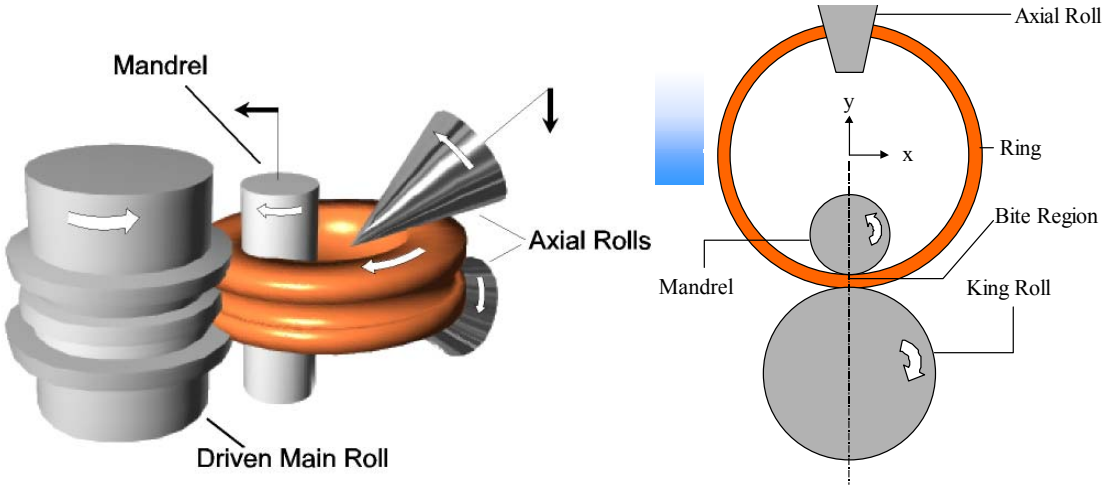

(a) *(b)*

Figure 1: (a) 3-D View of ring rolling process, (b) Schematic of ring rolling process

Parts produced by the ring rolling process can be quite complex, as demonstrated in *Figure 2*. The ring cannot generally be deformed or rolled to the final shape, with a desired ring diameter, in a single pass. To avoid problems such as foldovers, localized deformation, and improper roll fill, the workpiece (ring) should be deformed into one or more intermediate shapes before a product of the desired shape is obtained. The proposed backward simulation technique helps the engineer avoid unnecessary internal shearing in an effort to obtain the desired final shape. An optimum intermediate shape ensures that the various cavities in the roll profile get filled simultaneously.

The main objective of this research is to develop an analytical method for the profile ring rolling process in order to establish a new approach to determine the intermediate shapes of the ring profile using UBET. Comparison of the UBET results against experimental results is also presented here to check the accuracy of the UBET results. There is no unique method of arriving at an intermediate shape because the only parameters known in advance are the final product shape, the final diameter of the ring, and the material with which it is to be made. Experimental data as well as previous experience also play a major role in deciding the appropriate intermediate shapes.

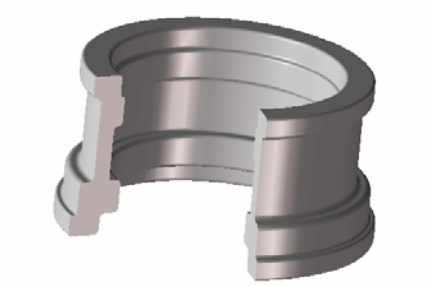

Figure 2: Actual ring geometry

The upper bound theorem was formulated by Prager and Hodge [4] and later modified by Drucker, et al. [5,6] to include the presence of velocity discontinuities. Several applications of the upper bound method to metal forming problems have appeared in the literature over the years. Kudo [7] introduced the concept of dividing the deforming material into unit deformation blocks to obtain the best upper bounds by a suitable choice of the shape and number of the these unit blocks. Kobayashi [8] suggested curved discontinuity surfaces for the unit regions, which resulted in better upper bounds for some axisymmetric forming problems. Preform design by the three-dimensional finite method has been carried out for plain ring rolling and T-section profile ring rolling by Kobayashi et al. [9]. Kobayashi et al. [10] also used the method of backward tracing of deformation processes and has applied it successfully to preform design in metal forming. Bramley et al [11] successfully used UBET for modeling several manufacturing processes, such as closed-die forging and extrusion. Also, Bramley [12] used UBET and tetrahedral upper bound analysis (TEUBA) as fast methods for forging simulation and preform design. Bramley concluded that UBET and TEUBA have capabilities that offer complementary

advantages when compared with the currently used FEM. Davey et al. [13] described measures that make the analysis of ring rolling a practicable proposition. Also, Davey et al. [14] examined the computational performance of an arbitrary Lagrangian-Eulerian (ALE) flow formulation for ring rolling in combination with the successive preconditioned conjugate gradient method (SPCGM). Qingbin et al. [15] presented a preform design method that combines the FEM-based forward simulation and the UBET-based reverse simulation techniques. Avitzur et al. [16] used both the upper bound method and UBET for modeling of extrusion with and without friction. Yang et al. [17] used the upper bound method to predict the roll torque in the rolling of L-section rings. Gunasekera and Jia have used UBET for the modeling of extrusion of simple profiles using the shear die. [18,19] Alfozan and Gunasekera [3,20] have compared UBET with a FEM package (DEFORM) for axisymmetric closed-die forging and have developed a simulation software tool for the ring rolling process based on UBET.

Theoretical Analysis

The basic concept of UBET is to break up the workpiece into a number of regions. *Figure 3* is an idealized representation of the actual cross-sectional geometry of the type shown in *Figure 2*, which is based on constant volume. However, the analysis is actually three-dimensional (or 2½-dimensional because the circumferential or z velocity is identical for all elements). *Figure 4* shows the actual ring with king and mandrel rolls, the cross-section geometry is shown in *Figure 3*. During the ring rolling process, the cross-sectional area of the ring reduces at each time step, resulting in a corresponding increase in diameter of the ring due to the material incompressibility. The material flows across the boundary of an element into its neighboring element, while satisfying volume constancy. The objective of formulating the UBET is to minimize the total energy rate, $\dot{W}_{tot}$, of all the elements constituting the workpiece. Moreover, a kinematically admissible velocity field is constructed for each element during each time step. The total consumption of energy is calculated by summing up the consumption values for all the elements. The upper bound on the total energy rate is computed by considering (a) the internal homogeneous deformation throughout the deforming zone, (b) the energy dissipated due to discontinuities across the internal shear surfaces, and (c) the frictional loss over the tool-material interface. The optimal solution is obtained by minimizing the total energy rate with respect to the unknown parameters in the velocity field inside the deforming region. Refer to Alfozan's dissertation [21] for more details of the analysis method.

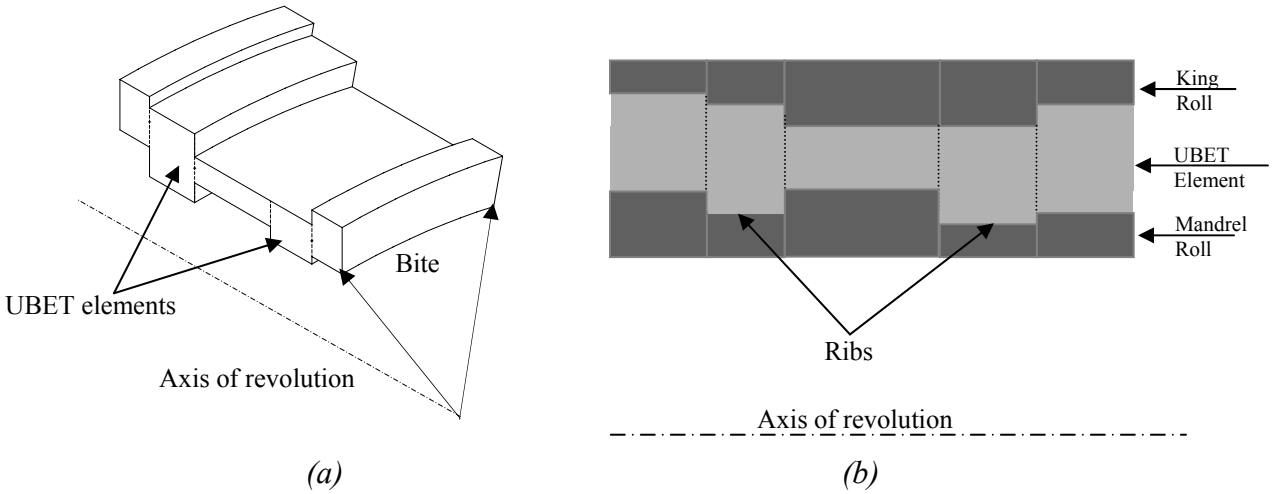

Figure 3: (a) Cutaway section of ring, (b) UBET idealization of rolls and ring

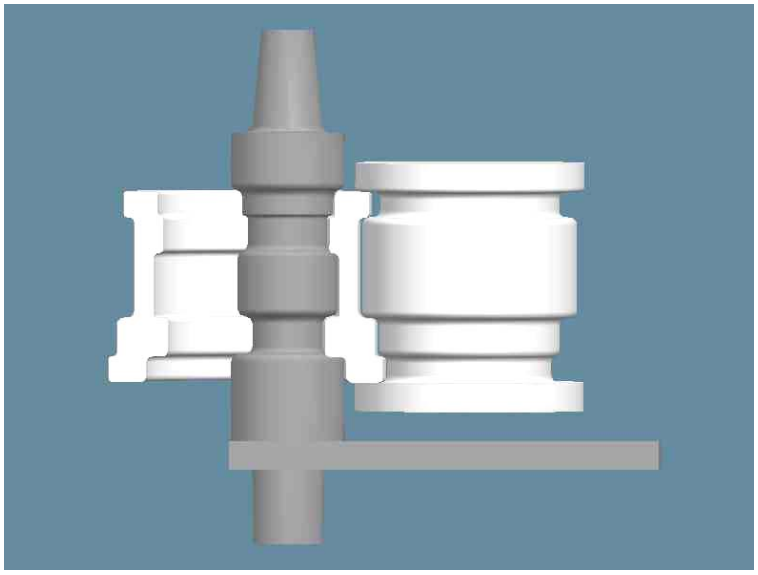

Figure 4: Actual ring with king and mandrel rolls

Assumptions

The theoretical model is based upon the following assumptions:

1. The velocity is uniformly distributed on the UBET element boundary surfaces.
2. Velocities, u, v, and w are linearly varied within each UBET element along the coordinate directions (see *Figure 5*).
3. The elastic deformation is small compared to the plastic deformation and is therefore neglected.
4. The material is isotropic, homogeneous, rigid-plastic, and obeys the von Mises yield criterion.
5. The material is incompressible, satisfying the relation: $\dot{\varepsilon}_x + \dot{\varepsilon}_y + \dot{\varepsilon}_z = 0$, where $\dot{\varepsilon}_x, \dot{\varepsilon}_y$, and $\dot{\varepsilon}_z$ are the strain rates in the x, y, and z directions, respectively.
6. The frictional shear stress, τ, is expressed by a constant friction factor, m, according to the relation $\tau = mk = m\ \bar{\sigma}/\sqrt{3}$, where, k is the shear yield stress of the workpiece material.
7. The tools (rolls) are absolutely rigid, and bite length is straight.
8. The deformation in the z direction (that is, the circumference) is the same for all elements (that is, 2½-D).
9. Each roll pass is approximated by a forging step of appropriate stroke, that is, distance moves by mandrel during one revolution of the ring.
10. Small corner radii on the roll surface are neglected in the model.

Kinematically admissible velocity field

The most fundamental requirement for the application of UBET is the establishment of a kinematically admissible velocity field. The velocity field for each ring element (of rectangular cross section) is derived by satisfying the external boundary conditions, the normal velocity-continuity condition at the interfaces between adjacent elements, and the volume-constancy condition $\dot{\varepsilon}_x + \dot{\varepsilon}_y + \dot{\varepsilon}_z = 0$. The entire surface of an element is allowed to suffer plastic flow. In addition, it is assumed that normal velocity at the boundary of an element is distributed uniformly over each part of the surface. The x, y, and z components of the velocity field (u, v, w) in a typical element may be written as

$$\begin{aligned} u &= a_1 x + b_1; \\ v &= a_2 y + b_2; \\ w &= a_3 z + b_3; \end{aligned} \qquad (1)$$

where a_i and b_i are constant coefficients that can be determined by using the boundary conditions. According to the incompressibility condition, $\dot{\varepsilon}_x + \dot{\varepsilon}_y + \dot{\varepsilon}_z = 0$, for a typical element shown in *Figure 5*, where the strain rates are given by;

$$\dot{\varepsilon}_x = \frac{\partial u}{\partial x}, \qquad \dot{\varepsilon}_y = \frac{\partial v}{\partial y}, \qquad \dot{\varepsilon}_z = \frac{\partial w}{\partial z} \tag{2}$$

Integrating Eq. (2) with the boundary conditions, the general kinematically admissible velocity field for a rectangular element can be expressed as:

$$\begin{aligned} u &= u_{i,j,k} - \frac{(u_{i,j,k} - u_{i+1,j,k})}{(x_i - x_{i+1})} x_i + \frac{(u_{i,j,k} - u_{i+1,j,k})}{(x_i - x_{i+1})} x \\ v &= v_{i,j,k} - \frac{(v_{i,j,k} - v_{i,j+1,k})}{(y_i - y_{i+1})} y_j + \frac{(v_{i,j,k} - v_{i,j+1,k})}{(y_i - y_{i+1})} y \\ w &= w_{i,j,k} - \frac{(w_{i,j,k} - w_{i,j,k+1})}{(z_i - z_{i+1})} z_k + \frac{(w_{i,j,k} - w_{i,j,k+1})}{(z_i - z_{i+1})} z \end{aligned} \tag{3}$$

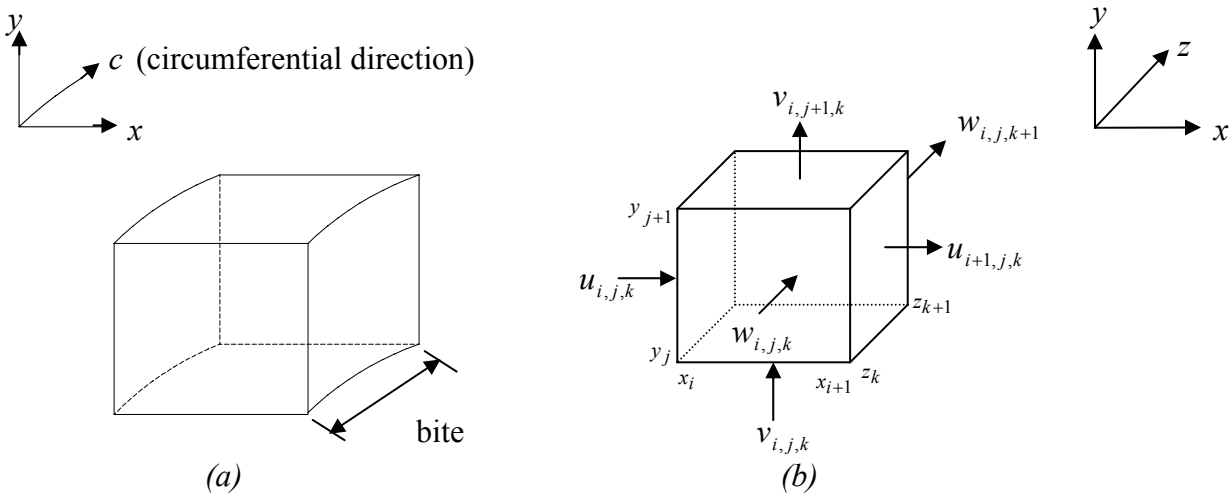

Figure 5: (a) Actual element, (b) Rectangular (ring) element approximated

Total power dissipation

To determine the optimal velocity field, the total power dissipation $\dot{W}_{tot}$ is minimized with respect to all the unknown variables, which are the velocity components distributed on bounding surfaces of the rectangular elements.

The upper-bound solution is obtained using the derived velocity field for each step during the rolling process. The total energy rate of dissipation for the proposed velocity field is given as

$$\dot{W}_{tot} = \sum \dot{W}_p + \sum \dot{W}_s + \sum \dot{W}_f \tag{4}$$

where $\dot{W}_p$ is the power dissipation due to pure plastic deformation over a deforming volume (UBET element) and can be expressed as,

$$\dot{W}_p = \int_v \bar{\sigma}\,\dot{\bar{\varepsilon}}\,dv \tag{5}$$

$\dot{W}_s$ is the power dissipation due to the velocity discontinuities (internal shear) across the boundaries between UBET elements and can be defined as:

$$\dot{W}_s = \int_s \tau \left|\Delta W_s\right| ds = k\int_s \left|\Delta W_s\right| ds \tag{6}$$

$\dot{W}_f$ is the power dissipation due to friction at the interfaces between ring and roll and it is defined as

$$\dot{W}_f = \int_s \tau \left|\Delta W_f\right| ds = m\int_s k \left|\Delta W_f\right| ds \tag{7}$$

Each component of the power dissipation is a function of the velocities of the bounding surfaces of the rectangular element. These unknown velocities are determined by minimizing the total power dissipation. The geometry of each UBET element is then updated. Therefore, the new boundaries of each element after a time increment Δt for backward simulation are given by:

$$\begin{aligned} x_i(t-\Delta t) &= x_i(t) - U_x\,\Delta t \\ y_i(t-\Delta t) &= y_i(t) - U_y\,\Delta t \\ z_i(t-\Delta t) &= z_i(t) - U_z\,\Delta t \end{aligned} \tag{8}$$

where $x_i(t)$, and $x_i(t-\Delta t)$ are the coordinates of the UBET element in x-direction at time steps t and $t-\Delta t$, respectively, and U_x is the corresponding component of the velocity normal to the surface of the element in the optimal velocity field at time step t. The y, and z coordinates of the displaced element are calculated similarly.

Results and Discussion

In an attempt to arrive at intermediate shapes systematically, a method based on backward simulation is proposed. This method utilizes the energy variations that occur during the deformation of the material. The fundamental aim is to identify the lowest energy rate during the deformation of the material for the possible cases of contact of the ring with the roll cavity.

A systematic method to identify the minimum energy rate during the process is achieved by considering each and every rib filling the roll cavity. When the rib is not in contact with the base of the roll cavity (that is, free), the UBET will recognize this rib as a region having an unknown velocity. When the base of the roll cavity is in contact with a rib, the velocity of that rib will be equal to the velocity of the roll during the ring rolling process. These two cases help to identify the lowest energy consumption for the ring roll process.

As shown in *Figure 3*, there are six free surfaces (that is, ribs with no roll contact) for the element cross section. The possible combinations between free (i.e., f) and rolls contact (i.e., v) are 63 ($2^6 - 1 = 63$). All the possible combinations were tested in order to identify the lowest energy during the ring rolling process; some of the combinations and their associated energy rates are shown in *Figure 6*. The energy rate corresponding to free (no contact with rolls) simulation was found to be the lowest during the backward simulation of ring roll process using UBET. Therefore, the strategy to achieve the intermediate shape is based on keeping all the ribs free (the roll cavities are unfilled). The backward simulation will stop when the inner edge of any of the ribs is in line with that of the adjacent element that has been in contact with the rolls since the beginning of simulation. However, the optimal design of metal flow and roll fill in order to roll the workpiece is achieved when the flow of the material fills up all roll cavities at approximately the same time. If the cavities are filled prematurely, there is a possibility that they may get unfilled with further expansion of the ring.

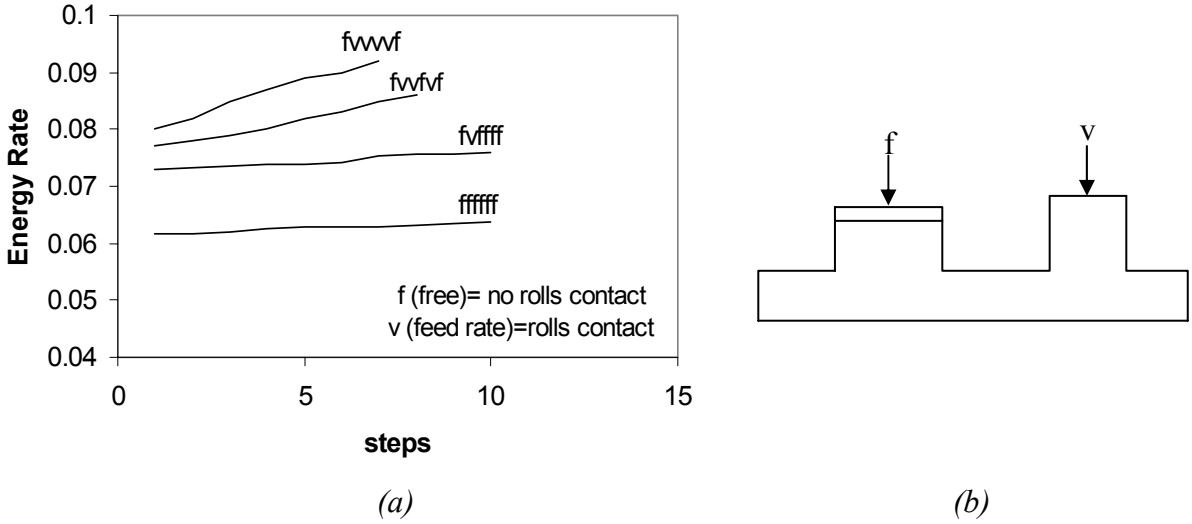

Figure 6: (a) Behavior of energy rate, (b) Identification of free surface (f) and rolls contact (v)

Undeformed and deformed shapes by backward simulation

During the ring rolling process (forward simulation) the cross-sectional area of the ring reduces at each time step, resulting in an increase in diameter of the ring. In the backward simulation of profile ring rolling, on the other hand, the cross-sectional area of the ring increases at each time step with a corresponding reduction in diameter of the ring. Different kinds of profiles were taken as test cases of the profile ring rolling. Two of the test cases are explained in detail in this paper. In the first case, roll cavities were considered for the main and mandrel, while in the second case a flat main roll was considered. The mandrel roll was utilized in this work with a feed rate of 0.01 in./sec, and the rotation speed for the king roll was 50 rpm. The interface lubrication was representative of a friction factor of 0.3.

The sequence of steps followed in the backward simulation of the profile ring rolling using UBET is shown in *Figure 7*, which indicates the final geometry of forward simulation. As shown in *Figure 7*, the ring was progressively released from the main and mandrel rolls by increasing the cross-sectional area of the ring and reducing its diameter at each time step using the condition of volume constancy. The simulation was stopped when the height of element 5 was equal to that of element 3, which had been in contact with the roll since the beginning of the process. This represents an ideal preformed shape of the ring, and the procedure can be repeated with fewer ribs (that is, four ribs and then three ribs, and so on).

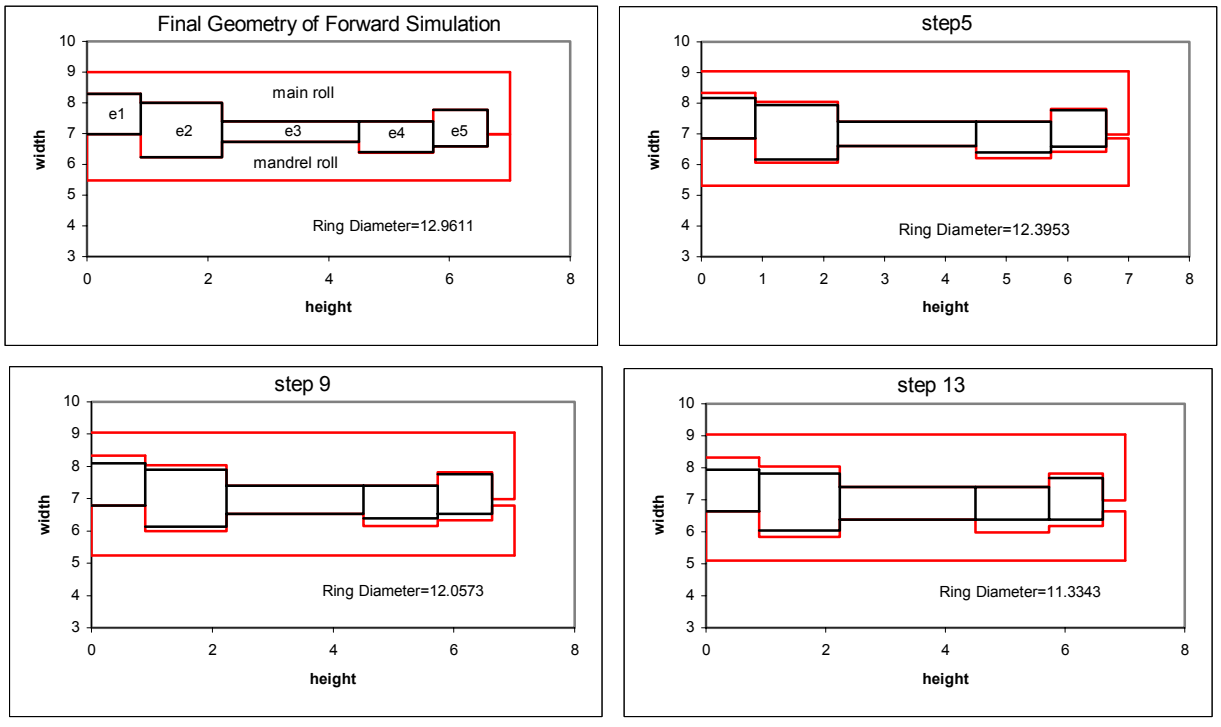

Figure 7: Sequence of shapes during ring rolling by backward simulation using UBET for 5 elements

Experimental results

The experimental work has been carried out to validate the computed results of the backward simulation using UBET. This was done on the ring rolling mill that has been designed and fabricated in the Dept. of Mechanical Engineering at Ohio University for investigation and validation purposes. It turns out to be the only existing ring rolling mill in any university in the United States. In the present experimental work, only a grooved mandrel was employed for minimizing the cost and time of machining. The main components of the radial ring-rolling configuration are shown in *Figure 8*.

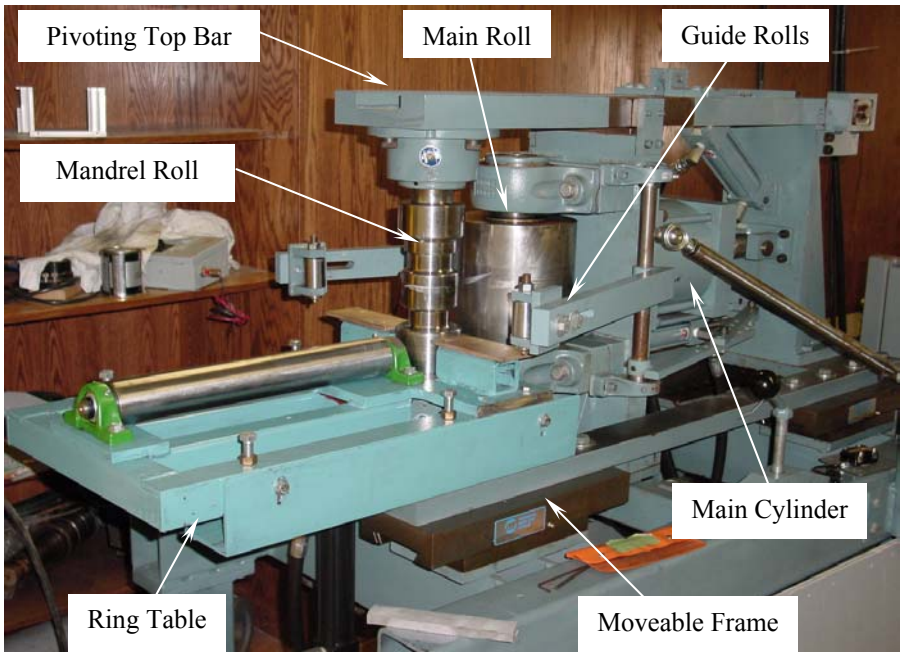

Figure 8: Ring rolling machine at Ohio University

The radial ring-rolling machine is capable of rolling rings with initial diameters of 5-7 in. up to maximum of 15 in., with 2 in. minimum wall thickness and 6 in. maximum height. The chief characteristics of the main roll are that it is 8 in. in diameter, has a motor power of 20 hp, and a 50 rpm maximum speed. The diameter of the mandrel roll is 4 in. with a maximum horizontal force of 17,500 lb. The feed rate can be adjusted to lie within 0.009-0.254 in./sec. *Table 1* summarizes the process and geometrical parameters used in the analysis. The experiment was performed with aluminum 1050 (at 570° C initial billet temperature).

The diametral growth of the ring during profile ring rolling is displayed by a sequence of steps in *Figure 9*. The material flows outward to form the web into the cavities of the mandrel roll, causing a simultaneous increase in diameter of the ring and an associated reduction in the cross-sectional area at each time step of the operation. *Figure 10* shows the final shape of the fully deformed ring with a progressive growth of the ring diameter with continuous profile formation. A cross section of the completely deformed ring is shown in *Figure 11*.

Table 1: Process parameters

Main roll diameter	8 in.
Mandrel roll diameter	4 in.
Speed of main roll	50 rpm
feed of pressure roll	0.01 in./time
Friction factor, *m*	0.3
Material	Aluminum 1050
Initial Temperature	570° C
Initial ring outer-diameter	8 in.
Initial ring inner-diameter	4.15 in.
Initial ring height	6.5 in.

Figure 9: Deformed configurations at selected times

(a) *(b)*

Figure 10: (a) Rings produced, (b) Compared with initial workpiece

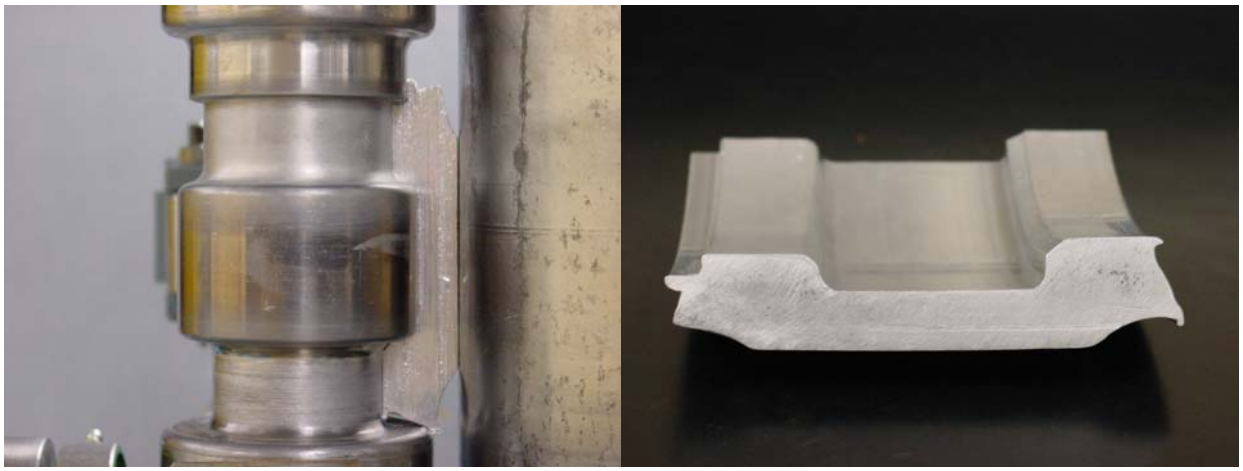

(a) *(b)*

Figure 11: (a) Cross section of fully deformed ring, (b) Cross section of final product

Comparison between UBET and experimental results

The validation is an essential part of any metal forming analysis, for it helps to determine the accuracy of the results that the analysis is capable of producing. A comparison is made between the experimental results and the new approach of the backward simulation using UBET for the profile ring rolling process in relation to the filling of grooves in the mandrel roll, as well as the growth of the ring diameter.

In the present experimental work, only the grooved mandrel with flat main roll was employed for minimizing the cost and time. *Figure 12* shows the sequence of steps followed in the simulation of the profile ring rolling by backward simulation using UBET with the same conditions and parameters (geometry, feed rate, and so on) as those employed in the experimental work. As shown in *Figure 12*, the ring progressively released the cavities of the grooved mandrel roll by increasing the cross-sectional area of the ring and reducing its diameter at each time step while matching volume constancy. The simulation was stopped when the height of element 1 and 3 were equal to that of the horizontal part of element 2, which had been in contact with the roll since the beginning of the process.

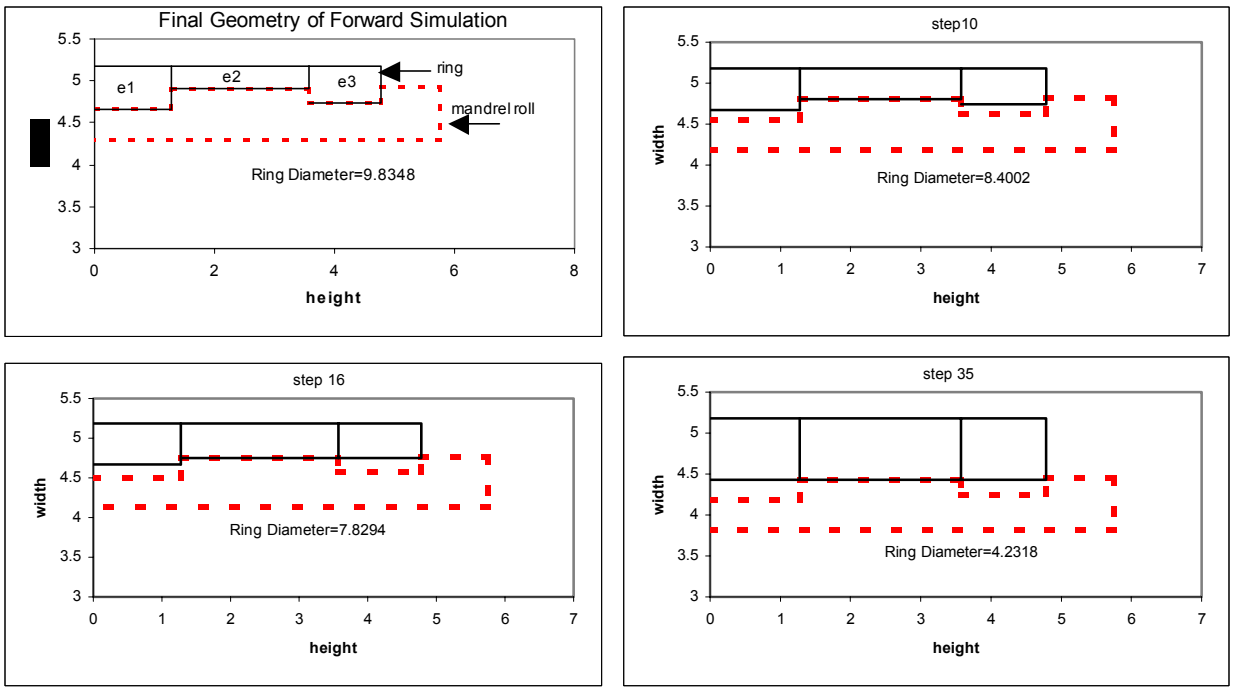

Figure 12: Sequence of shapes during ring rolling by backward simulation using UBET for 3 elements

A comparison between the backward simulation using UBET and experimental results can be seen in *Figure 13*. As expected in ring rolling with high reduction rates, the ring experienced uneven side spread across the cross section. In practice, these types of reduction rates are typically applied with the help of axial rolls that control the side spread (maintaining the rectangular shape of the cross section). The experimental results that were obtained by using only radial rolls (without axial rolls) indicated that the material expansion on the ring height was fairly small. Consequently, attempts were made to get the results without axial rolls. Both sides of the ring have been assumed to be constrained in the theoretical treatment. The theoretical and experimental results in terms of growth rate of the ring diameter for each element are summarized in *Table 2*. The percentage error between the UBET and experimental results in relation to the matching the ring thickness (at the web thickness) has been found to lie in the

range 7.5%-8.5%. The UBET results therefore compared very well with the experimental results. The error may be attributed to the fact that rectangular elements in UBET are not able to match the ring cross section exactly. Consequently, the UBET approach seems to be an acceptable method for the simulation of profile ring rolling.

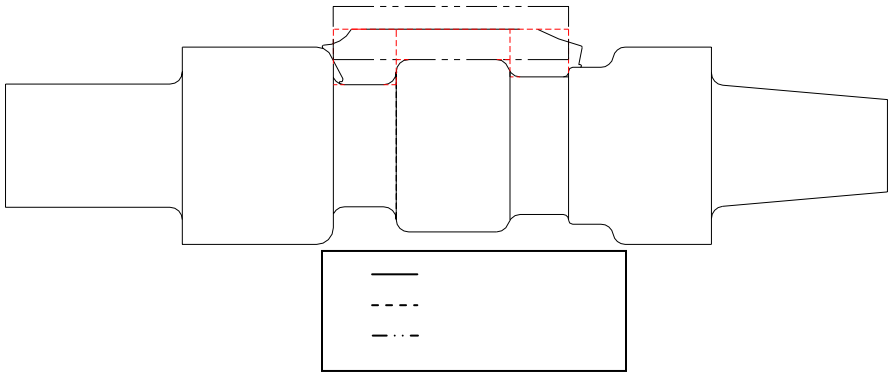

Figure 13: Comparisons between UBET and experimental results

Table 2: Comparisons between UBET and experimental results for ring diameters

	Element 1		**Element 2**		**Element 3**	
	ID	**OD**	**ID**	**OD**	**ID**	**OD**
UBET (1 min.)	8.46 in.	9.56 in.	8.96 in.	9.56 in.	8.61 in.	9.56 in.
Experimental (4 min.)	9.25 in.	10.34 in.	9.74 in.	10.34 in.	9.37 in.	10.34 in.
Error% $\frac{Th. - Exp.}{Exp.}$	8.54	7.54	8.00	7.57	8.11	7.54

Conclusions

Due to the complex nature of the ring rolling process, no analytical method can exactly solve the process of the backward simulation to determine the optimum intermediate shapes of the ring profile. The plastic flow of material in ring rolling may be envisaged as a sequence of successive closed-die forging processes. This assumption made it easier to analyze the process. The lowest energy rate is the key issue to achieve the optimum intermediate shape. UBET (forward

simulation) provides fairly accurate but quick results for profile ring rolling. The UBET (backward simulation) is capable of providing near optimum intermediate shapes. The limitation of the current UBET simulation is that it can only handle rectangular elements with sides parallel to x and y axes. It is important to note that the FEM technique cannot easily simulate the profile ring rolling process through either forward or backward simulation. Several FEM codes that could solve large plastic deformation problems were considered for ring rolling, but they proved to be inadequate for the complex rotation boundary condition at the roll/ring interface. Even if one was successful, it would take a very large number of time steps, involving several weeks to complete the process. UBET typically takes few minutes of computing time on a PC. However, there is no unique method of arriving at an intermediate shape, because the only parameters known beforehand are the final product shape, the final diameter of the ring, and the material with which it is to be made. Experimental data and previous experience play a major role in deciding the appropriate intermediate shapes. When one cavity is filled, the material subsequently flows toward another roll cavity, causing intense shearing between the dead zone (or the slow moving material) and the moving material. In the optimal design of the process, the material flows in such a way as to fill up all roll cavities at nearly the same time with the lowest energy dissipation. The backward simulation technique will help the engineer to avoid the possibilities of foldovers, localized deformation, unwanted internal shearing and improper roll fill, while simultaneously trying to attain the final ring shape with the desired final ring diameter. UBET predictions compared very favorably with experimental results. As the results indicated, the proposed method is capable of solving geometrically complex ring-rolling problems using a small number of simple UBET elements.

References

1. A. Kluge, Y. Lee, H. Wiegels, and R. KOPP, "Control of Strain and Temperature Distribution in the Ring Rolling Process," *Journal of Materials Processing Technology* (v45, 1994), p.137.
2. D. Yang, K. Kim, and J. Hawkyard, "Simulation of T-Section Profile Ring Rolling by the 3-D Ring-Plastic Finite Element Method," *Int. J. Mech. Sci.* (v7, 1991), p.541.
3. A. Alfozan and J. Gunasekera, "Computer Simulation of Profile Ring Rolling," *5th International Conference on Engineering Design and Automation* (Las Vegas, 2001), p.428.
4. W. Prager and P. Hodge, "Theory of Perfectly Plastic Solids," John Wiley and Sons, Inc. (1951).
5. D. Drucker, H. Greenberg, and W. Prager, "The Safety Features of and Elastic-Plastic Body in Plain Strain," *Trans. ASME, Journal of Applied Mechanics* (v73, 1951), p.371.
6. D. Drucker, W. Prager, and H. Greenberg, "Extended Limit Design Theorems for Continuous Media," *Quarterly of Applied Mathematics* (v9, 1952), p.381.
7. H. Kudo, "An Upper Bound Approach to Plane Strain Forging and Extrusion," *International Journal of Mech. Sciences* (Parts I and II, 1959), p.229.
8. S. Kobayashi and E. Thomsen, "Upper and Lower Bound Solutions to Axisymmetric Compression and Extrusion Problems," *International Journal of Mechine Sciences* (v7, 1965), p.127.

9. B. Kang and S. Kobayashi, "Preform Design in Ring Rolling Processes by the Three-Dimensional Finite Element Method," *International Journal of Machine Tools & Manufacture* (v30, 1991), pp.139-151.
10. S. Hwang and S. Kobayashi, "Preform Design in Shell Nosing at Elevated Temperatures," *International Journal of Machine Tools & Manufacture* (v27, 1987), pp.1-14.
11. A. Bramley, "Computer Aided Forging Design," *Annals of the CIRP* (v36, 1987), p.135.
12. A. Bramley, "UBET and TEUBA: Fast Methods for Forging Simulation and Preform Design," *Journal of Materials Processing Technology* (v116, 3 Oct. 2001), pp.62-66.
13. M. Ward and K. Davey, "A Practical Method for Finite Element Ring Rolling Simulation Using the ALF Flow Formulation," *International Journal of Mechanical Sciences* (v 44, Jan. 2002), pp.165-190.
14. K. Davey and M. Ward, "An Efficient Solution Method for Finite Element Ring-Rolling Simulation," *International Journal for Numerical Methods in Engineering* (v47, April 2000), pp.1997-2018.
15. Q. Liu, S. Wu, and S. Sun, "Preform Design in Axisymmetric Forging by a New FEM-UBET Method," *Journal of Materials Processing Technology* (v74, Feb. 1998), pp.218-222.
16. B. Avitzur, "Metal Forming Processes and Analysis," McGraw-Hill, New York, (1968).
17. D. Yang, J. Ryoo, J. Choi, and W. Johnson, "Analysis of Roll Torque in Profile Ring Rolling of Aluminum Bicycle Wheel Rims," *Int. J. Mech. Sci*. (v28, 1986), p.841.
18. Z. Jia, "An Integrated Analysis and Design Method for Metal Forming Processes," Ph.D. dissertation thesis (Ohio University, March 1998).
19. J. Gunasekera, Z. Jia, and J. Malas, "Analysis of Aluminum Extrusion Processes Using Upper Bound Element Technique," *Proc. Third World Conf. On Integrated Design and Process Technology* (Berlin, Germany, 1998), p.215.
20. A. Alfozan and J.S. Gunasekera, "An Upper-Bound Elemental Technique Approach to the Process Design of Axisymmetric Forging by Forward and Backward Simulation," *Journal of Materials Processing Technology,* (to appear).
21. A. Alfozan, "Development and Validation of UBET for Forward and Backward Ring Rolling Process," Ph.D. dissertation (Ohio University, to appear).
22. Z. Wang, K. Xue, and Y. Liu, "Backward UBET Simulation of the Forging of a Blade," *Materials and Processes in Manufacturing* (1995).
23. G. Zhao, E. Wright, and R. Grandhi, "Forging Preform Design with Shape Complexity Control in Simulating Backward Deformation," *International Journal of Machine Tools Manufacturing* (v35, 1995), p.1225.
24. Y. Hahn and D. Yang, "UBET Analysis of the Closed-Pass Ring Rolling of Rings Having Arbitrarily Shaped Profiles," *Journal of Materials Processing Technology* (v40, 1994), p.451.
25. J. Hou, "A Plan-Strain UBET Analysis of Material Flow in a Filled Deep Die Cavity in Closed-Die Forging," *Journal of Materials Processing Technology* (v62, 1996), p.81.
26. C. Xie, X. Dong, and S. Li, "Rigid-Viscoplastic Dynamic Explicit FEA of the Ring Rolling Process," *International Journal of Machine Tool and Structures* (v40, Oct. 2000), pp.81-93.
27. M. Joun, J. Chung, and R. Shivpuri, "An Axisymmetric Forging Approach to Preform Design in Ring Rolling Using A Rigid-Viscoplastic Finite Element Method," *International Journal of Machine Tools & Manufacture* (v38, Oct.-Nov. 1998), pp.1183-1191.